Nesprin-2 mediated nuclear trafficking and its clinical implications

Pranav Kelkar[1,2,3], Anna Walter[4], Symeon Papadopoulos[4], Carmen Mroß[1,2,3], Martina Munck[1,2,3], Vivek S Peche[1,2,3], and Angelika A Noegel[1,2,3,*]

[1]Institute for Biochemistry I; Medical Faculty; University of Cologne; Köln, Germany; [2]Cologne Excellence Cluster on Cellular Stress Responses in Aging-Associated Diseases (CECAD); University of Cologne; Köln, Germany; [3]Center for Molecular Medicine; University of Cologne; Köln, Germany; [4]Institute of Vegetative Physiology; Medical Faculty; University of Cologne; Köln; Germany

Nuclear translocation of proteins has a crucial role in the pathogenesis of cancer, Alzheimer disease and viral infections. A complete understanding of nuclear trafficking mechanisms is therefore necessary in order to establish effective intervention strategies. Here we elucidate the role of Nesprin-2 in Ca^{2+}/Calmodulin mediated nuclear transport. Nesprin-2 is an actin-binding nuclear envelope (NE) protein with roles in maintaining nuclear structure and location, regulation of transcription and mechanotransduction. Upon depletion of Nesprin-2 using shRNA, HaCaT cells show abnormal localization of the shuttling proteins BRCA1 and NF-κB. We show that their nuclear transport is unlikely due to the canonical RAN mediated nuclear import, but rather to a RAN independent Ca^{2+}/Calmodulin driven mechanism involving Nesprin-2. We report novel interactions between the actin-binding domain of Nesprin-2 and Calmodulin and between the NLS containing region of BRCA1 and Calmodulin. Strikingly, displacing Nesprins from the NE resulted in increased steady state Ca^{2+} concentrations in the cytoplasm suggesting a previously unidentified role of Nesprins in Ca^{2+} regulation. On comparing Nesprin-2 and BRCA1 localization in the ovarian cancer cell lines SKOV-3 and Caov-3, Nesprin-2 and BRCA1 were localized to the NE envelope and the nucleus in SKOV-3, respectively, and to the cytoplasm in Caov-3 cells. Fibroblasts obtained from EDMD5 (Emery Dreifuss muscular dystrophy) patients showed loss of Nesprin-2 from the nuclear envelope, corresponding reduced nuclear localization of BRCA1 and enhanced cytoplasmic Ca^{2+}. Taken together, the data suggests a novel role of Nesprin-2 in Ca^{2+}/Calmodulin mediated nuclear trafficking and provides new insights which can guide future therapies.

Introduction

The nuclear envelope (NE) presents as a physical barrier to the free shuttling of macromolecules to and from the nucleus. A finely regulated import and export machinery is therefore crucial for cellular processes like DNA damage response, inflammation and tumorigenesis. Proteins that undergo nucleo-cytoplasmic shuttling usually possess a nuclear localization sequence (NLS) and/or nuclear export sequence (NES). These sequences are then recognized by karyopherins which along with Ran and nucleoporins constitute the classical Ran dependent protein trafficking. In addition to this relatively well described pathway, nuclear shuttling proteins also employ a Ca^{2+}/Calmodulin mediated mechanism in regulating the localization of NLS containing proteins which is conserved from yeast to man.[1,2] The NLS of proteins such as Grb7, the NF-κB family proteins RelA and c-Rel, nuclear myosin NM1, SRY and SOX9 bind to Calmodulin and the binding has been suggested to play a role in nuclear localization of these proteins and can act either by promoting or inhibiting the import.[3–9] On the other hand, a change in intracellular

Ca^{2+} has an effect on nuclear import of NLS containing proteins such as Smad3, BRCA1 and p65.[10–12] Moreover, a change in intracellular Ca^{2+} is also important for nuclear export of proteins such as BRCA1, HDAC4, HDAC5 and the glucocorticoid receptor.[13–17] Sweitzer and Hanover (1996) attempted to assimilate the combined role of Ca^{2+} and Calmodulin in nuclear transport in a model where upon a stimulus for nuclear transport Ca^{2+} is released from the local stores, namely the NE and the endoplasmic reticulum (ER), and binds to Calmodulin. The activated Ca^{2+}/Calmodulin complex recognizes the NLS of the target molecule.[18] This tertiary protein complex is recognized by an unknown component of the NE and is internalized. However, the role of the NE in Ca^{2+}/Calmodulin mediated nuclear transport remained to be explored.[2,18] The apparent contradiction in the literature in the directionality of nuclear transport in response to Ca^{2+} release may be explained by the levels of free Ca^{2+} in the resting and stimulated state of a given cell type.[18]

Nesprin-2 is an actin-binding NE protein that links the nucleoskeleton to the cytoskeleton. It comprises an N terminal actin-binding domain (ABD) composed of 2 Calponin homology
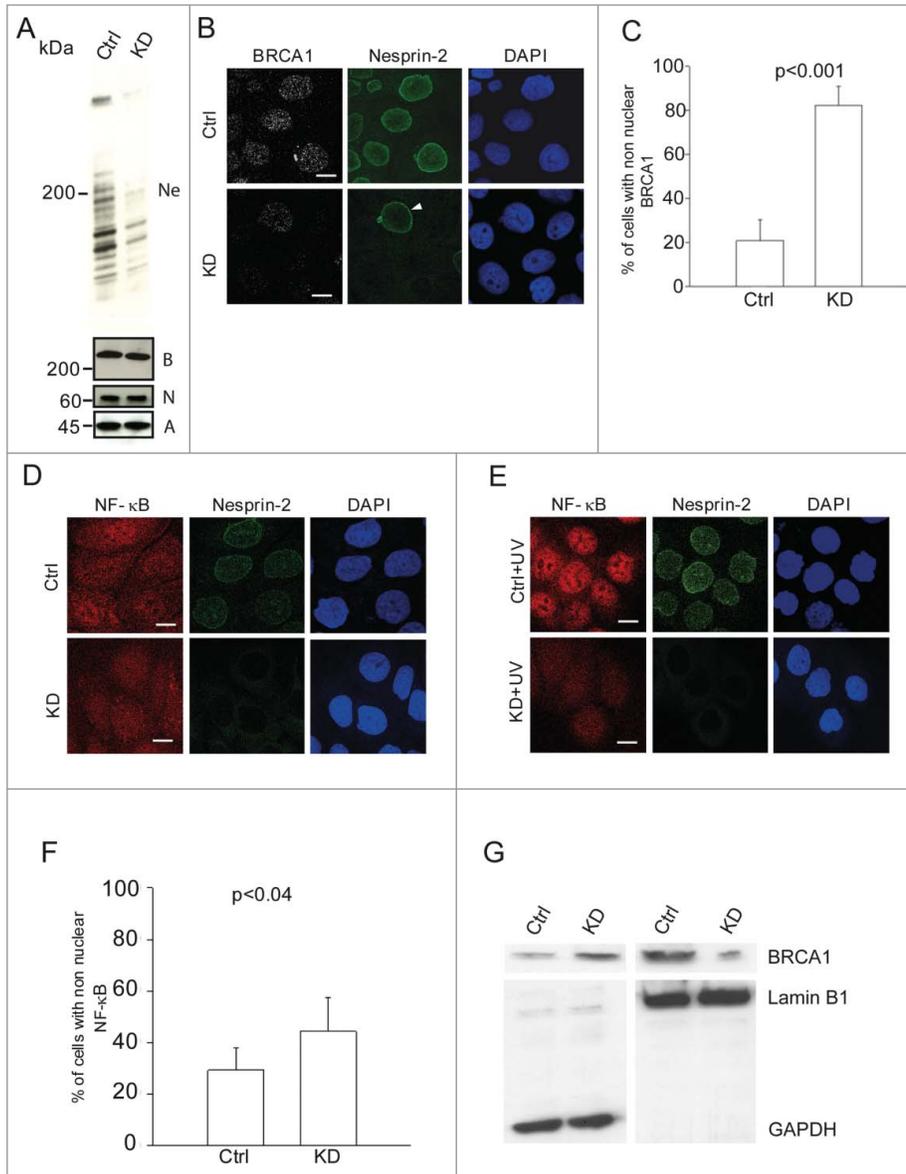
Figure 1. Reduced nuclear localization of BRCA1 and NF-κB in Nesprin-2 knockdown (KD) HaCaT cells and its effect on UV induced DNA damage response. (**A**) Western blots showing Nesprin-2 (Ne), BRCA1 (B) and NF-κB (N) levels in whole cell lysates obtained from control (Ctrl) and Nesprin-2 KD cells. Nesprin-2 was detected with pAbK1. β-actin (A) detected with monoclonal antibodies was used for loading control. (**B**) Immunofluorescence study in control (Ctrl) and Nesprin-2 knockdown (KD) cells using BRCA1 (shown in gray scale) and pAbK1 anti-Nesprin-2 antibodies (shown in green). Arrowhead points at a control cell surrounded by Nesprin-2 KD cells. Scale bar, 10 μM. (C) Graphical representation of the percentage of cells with predominantly non-nuclear BRCA1 (mean ± s.d, p< 0.001). 200 cells were analyzed. (**D**) Distribution of NF-κB in control and knockdown cells in the absence of UV treatment. Staining was with polyclonal antibodies specific for NF-κB and mAb K20–478 against Nesprin-2. (**E**) Distribution of NF-κB in control and Nesprin-2 KD cells after UV treatment. Scale bar, 10 μm. (**F**) Graphical representation of the percentage of cells with predominantly non-nuclear NF-κB post UV treatment (mean ± s.d, p value, 0.0396). 200 cells were analyzed. (**G**) Subcellular fractionation of control and Nesprin-2 KD cells to reveal the distribution of BRCA1. The resulting blot was probed for BRCA1. Shown are the respective cytosolic (GAPDH positive) and nuclear fractions (Lamin B1 positive).

and vary in size and domain composition.[19] Nesprin-2 along with SUN proteins forms the LINC complex which is involved in mechanotransduction, transcriptional regulation, centrosomal positioning and cell polarization.[20–22] Nesprin-2 knockdown cells have a defective nuclear translocation of c-Fos and Smad 2/3.[23] However, the underlying mechanism of Nesprin-2 mediated nuclear transport is largely unknown.

Nesprin-2 mutations have also been linked to Emery-Dreifuss muscular dystrophy 5 (EDMD5), an autosomal dominant form of degenerative myopathy, in which the Nesprin-2β isoform composed of C-terminal spectrin repeats and the KASH domain carries a point mutation leading to amino acid exchange T89M.[24] This position is located in a spectrin repeat and is evolutionary highly conserved in all Nesprins. Intriguingly, the mutation leads to abnormal nuclear shape, mislocalization of nuclear envelope proteins and impaired protein-protein interactions. However, a tunable mechanism that results out of loss of Nesprin-2 and could be explored for therapeutics, has not been described in these patients. Moreover, Nesprin-1, another member of the Nesprin family of proteins, has been linked to cancer pathology.[25] Whether such a link between Nesprin-2 expression and cancer exists is an unsolved question. Elucidating the role of Nesprin-2 in tunable signaling cascades may lead to novel therapies and better understanding of the disease.

In this study, we tested the effects of Nesprin-2 depletion on the localization of NF-κB and BRCA1. We demonstrate that Nesprin-2 mediated nuclear transport follows a Ca^{2+}/Calmodulin dependent mechanism and has implications for abnormal localization for nuclear proteins in ovarian adenocarcinoma and in fibroblasts from an EDMD5 patient.

Results

Nesprin-2 knockdown cells have reduced nuclear localization of NF-κB and BRCA1

domains, multiple spectrin repeats and a C terminal KASH domain which anchors it in the nuclear membrane. Several isoforms have been identified that are derived from a single gene

To determine if Nesprin-2 mediated nuclear trafficking is specific to substrates c-Fos and Smad 2/3 only, we investigated the nuclear localization of BRCA1 and NF-κB in
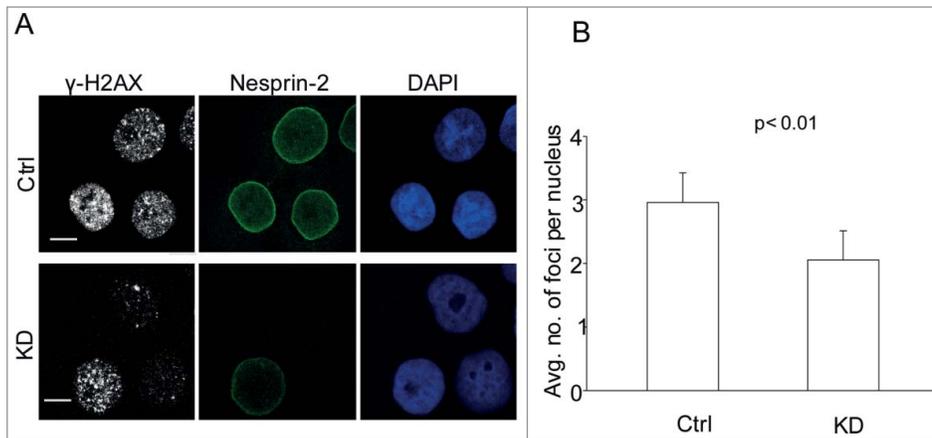
Figure 2. Nesprin-2 KD cells have a hypoactive DDR. (**A**) Immunofluorescence analysis after UV treatment of control and Nesprin-2 KD HaCaT cells with antibodies against Nesprin-2 (pAbK1), γ-H2AX and DAPI. Scale bar, 10 μm. (**B**) Graphical representation of the average number of γ-H2AX foci per nucleus. Foci ≥ 0.7 μm were counted, analysis was with cellprofiler image analysis software (mean ± s.d, p value, 0.0084). 100 cells were analyzed.

HaCaT cells in which Nesprin-2 was depleted by shRNA mediated knockdown (Nesprin-2 KD) as confirmed by Nesprin-2 specific pAbK1 (**Fig. 1A**).[26] BRCA1 is localized to the nucleus in untreated cells.[27] Upon Nesprin-2 depletion, which particularly affects the longer isoforms carrying the ABD, it is lost from the nucleus and diffusely distributed in the cytoplasm. We observed such a distribution in about 80% (p<0.05) of the KD cells, whereas cytoplasmic BRCA1 was seen in ~20% of the control cells (**Fig. 1B, C**). In contrast, NF-κB shows a diffuse nucleocytoplasmic distribution in control and Nesprin-2 KD cells (**Fig. 1D**). Upon UV treatment, NF-κB translocates to the nucleus in control cells whereas in Nesprin-2 KD cells, it maintains its nucleocytoplasmic distribution (**Fig. 1E**). Further analysis showed that after UV treatment NF-κB was present in the cytoplasm in ~25% of the control cells, whereas ~43% (p<0.05) of KD cells showed cytoplasmic NF-κB (**Fig. 1F**). The data thus suggest that Nesprin-2 mediated nuclear translocation is not specific for substrates c-Fos and Smad 2/3 but involves also BRCA1 and NF-κB. Cell fractionation of cytoplasmic and nuclear fractions of control and Nesprin-2 knockdown cells followed by western blotting also supports nuclear import deficiency upon Nesprin-2 depletion indicating that reduced nuclear localization of BRCA1 and NF-κB is not secondary to reduction in protein amount after Nesprin-2 knockdown (**Fig. 1G**, shown for BRCA1).

Furthermore, we evaluated the effect of abnormal nuclear trafficking on DNA damage response in Nesprin-2 KD cells since mobilization of proteins into the nucleus to repair damaged DNA is a key element in the DNA damage response (DDR). We used γ-H2AX as a marker. Because phosphorylation of H2AX at Ser 139 (γ-H2AX) is abundant, fast, and correlates well with DDR, it is the most sensitive marker that can be used to examine the DNA damage produced and the subsequent repair of the DNA lesion.[28] Nesprin-2 KD cells show reduced γ-H2AX foci formation in response to UV induced DNA damage, indicating a hypoactive DNA damage response presumably due to insufficient transport of essential repair proteins (**Fig. 2A, B**).
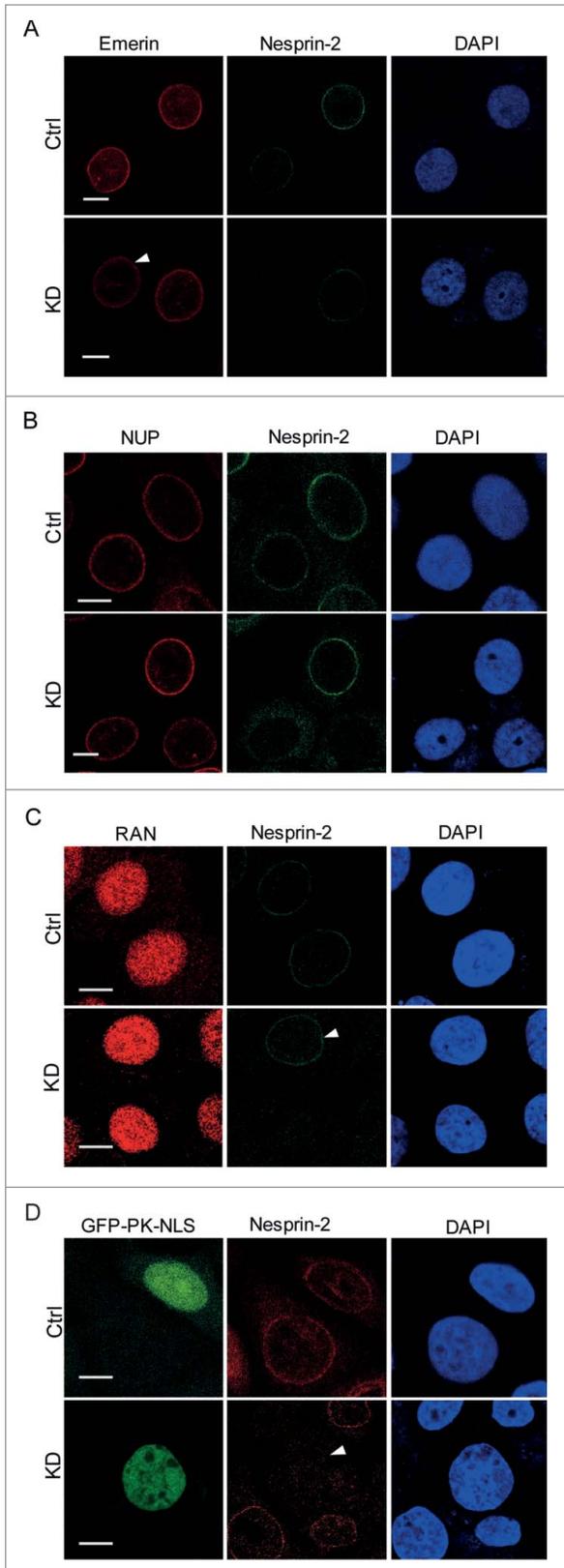
Nesprin-2 mediated nuclear trafficking is not secondary to loss of other nuclear envelope proteins and is RAN independent

Depletion of Nesprin-1 from the nuclear envelope results in reduction of Emerin at the nuclear envelope.[25] To investigate if Nesprin-2 depletion has a similar effect on Emerin which may then influence nuclear trafficking, we evaluated Emerin localization in Nesprin-2 KD cells by immunofluorescence analysis. In stark contrast to Nesprin-1, Nesprin-2 depletion did not affect Emerin localization suggesting that Nesprin-2 mediated nuclear trafficking is not secondary to loss of Emerin. Similarly, it did not affect the nuclear pore complex since Nesprin-2 knockdown cells did not show altered mAb414 staining (**Fig. 3A, B**). Also, the localization of RAN, a GTP-binding protein involved in nucleocytoplasmic transport, was not affected (**Fig. 3C**). To test if Nesprin-2 mediated nuclear translocation is RAN dependent, we probed the nuclear localization of GFP tagged to SV40 NLS since SV40 NLS is a well-documented cargo for importin mediated nuclear localization.[5,29] Nesprin-2 KD cells showed a nuclear localization of SV40 NLS similar to control cells indicating that Nesprin-2 mediated nuclear translocation is RAN independent (**Fig. 3D**).

Calmodulin interacts with the NLS containing region of BRCA1

Glover-Collins and Thompson (2008) demonstrated a novel Ca^{2+}/Calmodulin sensitive BRCA1 shuttling.[11] However, they did not test if the NLS of BRCA1 binds to Calmodulin. To investigate an interaction between BRCA1 and Calmodulin, we performed immunoprecipitation and GST pull down assays. COS7 cells were transfected with Calmodulin-YFP or YFP plasmid (negative control). Immunoprecipitation experiments performed using BRCA1 antibodies showed the presence of the ~45 kDa Calmodulin-YFP in the BRCA1 immunoprecipitate, indicating a novel interaction between BRCA1 and Calmodulin. YFP was not precipitated by BRCA1 antibodies (**Fig. 4A**). To further characterize the BRCA1 Calmodulin interaction, we used various GST constructs spanning the polypeptide sequence of BRCA1 (**Fig. 4B**). BRCA1 contains 2 NLSs in the region of amino acids 503–508 and 606–615 and one NES in the RING domain (amino acids 24–65). The polypeptides containing the NLSs and the RING domain were able to pull down Calmodulin-YFP but not YFP (**Fig. 4C**), indicating that the interaction between BRCA1 and Calmodulin is mediated by the NLS containing and also by the RING domain.

The interaction between Nesprin-2 and Calmodulin is mediated by the actin-binding domain of Nesprin-2

To investigate if Nesprin-2 could act as a nuclear envelope sensor to recognize Ca^{2+}/Calmodulin bound cargo for nuclear trafficking, we checked for an interaction between Nesprin-2 and Calmodulin using COS7 cells expressing Calmodulin-YFP (45 kDa) or YFP (28 kDa). In immunoprecipitation experiments performed with pAbK1 we found Calmodulin in the Nesprin-2 immunoprecipitate (Nesprin-2 IP) whereas YFP was not precipitated by Nesprin-2 antibodies indicating an interaction between Nesprin-2 and Calmodulin (**Fig. 5A**, middle panel).

The ABD of Nesprin-2 is highly homologous to the ABD of α-actinin.[30] This ABD has the potential to interact with Ca^{2+} binding EF-hands as they are present in Calmodulin.[31] Therefore we hypothesized that the ABD of Nesprin-2 can bind Calmodulin and carried out pull down assays with the His-tagged Nesprin-2 ABD (residues 1–285) and found that it could precipitate Calmodulin-YFP from cell lysates thus narrowing down the interaction site in Nesprin-2. In control experiments YFP was not precipitated by His-ABD (**Fig. 5A**, right panel, **B**). To test whether the interaction between the Nesprin-2 ABD and Calmodulin is direct or indirect, Calmodulin was expressed as GST-fusion protein, purified using glutathione-sepharose beads, eluted from the beads, dialyzed and incubated with Ni-NTA agarose carrying His-tagged ABD. GST was used for control. Bound proteins were analyzed by SDS PAGE analysis and staining with Coomassie Blue which revealed a direct interaction between the ABD and Calmodulin (**Fig. 5C**). In further experiments we added 2 mM $CaCl_2$ or 2 mM EGTA to the incubation buffer which showed that the binding occurred in the presence of Ca^{2+} but not in its absence (**Fig. 5D**). We also studied whether Nesprin-2 can interact with NF-κB and BRCA1 and found that they were immunoprecipitated from HaCaT cell lysates by Nesprin-2 pAbK1 antibodies (**Fig. 5E**).

Figure 3. Nesprin-2 knockdown does not affect the localization of Emerin, the nuclear pore complex, RAN, and the trafficking of SV40 NLS-GFP. (**A**) Immunofluorescence study of HaCaT control and Nesprin-2 KD cells using anti-Emerin and anti-Nesprin-2 antibodies (pAbK1). Arrow indicates a Nesprin-2 KD cell with emerin nuclear envelope localization. (**B**) Presence of nuclear pore proteins (NUP) at the NE as detected with mAb414. (**C**) Distribution of RAN. Immunofluorescence study using RAN (shown in red) and pAbK1 anti-Nesprin-2 antibodies (shown in green). Arrow indicates a control cell with Nesprin-2 nuclear envelope localization for comparison with surrounding KD cells. (**D**) Immunofluorescence analysis of double transfected cells either with Ctrl shRNA+GFP-PK-SV40 NLS or with Nesprin-2 shRNA+GFP-PK-SV40 NLS to detect localization of GFP-NLS in both control and Nesprin-2 KD cells. Nesprin-2 was detected with pAbK1. Arrow points to a KD cell having nuclear GFP-PK-SV40 NLS. Scale bar, 10 μm.
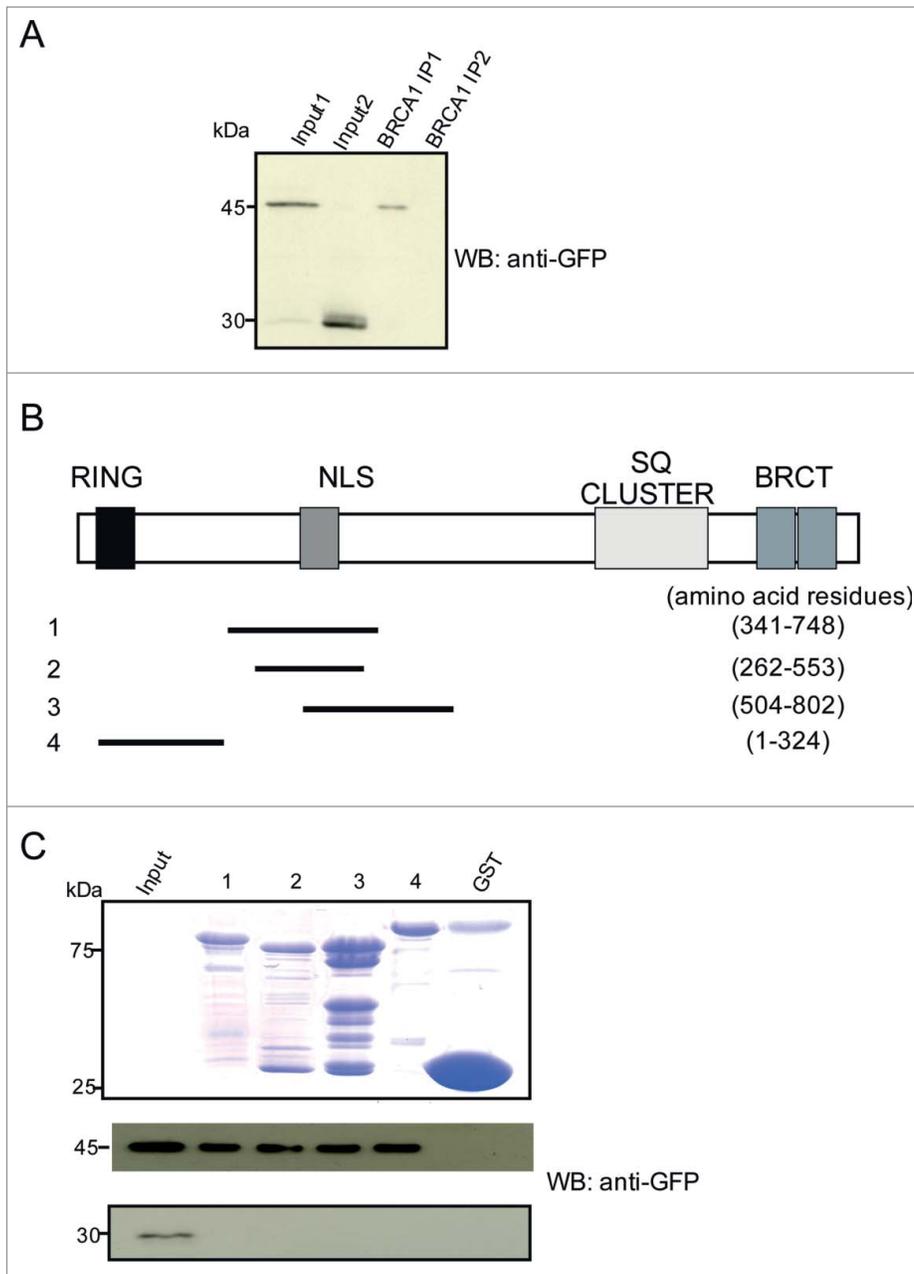
Figure 4. Calmodulin interacts with BRCA1 and the interaction is mediated via its NLS containing region. (**A**) Detection of YFP-Calmodulin in the BRCA1 immunoprecipitate. COS7 cells expressing YFP-Calmodulin (~45 kDa) were used. YFP-Calmodulin was detected using GFP-specific mAb K3–184–2. For the pulldown BRCA1 specific antibodies were used. YFP alone was not precipitated. Input 1 and 2 show the respective cell lysates containing YFP-Calmodulin and YFP used for pull down (IP1 and 2, respectively). (**B**) Position of peptides employed along the 1863 aa BRCA1 protein. The location of the domains of BRCA1 is indicated. (**C**) Detection of Calmodulin in pull downs using GST fusions of the indicated BRCA1 polypeptides. A Coomassie Blue stained gel shows the GST-fusion proteins. COS7 cells expressing YFP-Calmodulin were used. YFP-Calmodulin was detected by mAb K3–184–2. The lower panel shows the control pull down performed with lysates of cells expressing YFP only.

cellular Ca^{2+} levels, we performed live Ca^{2+} imaging using HaCaT cells expressing SP-GFP-SUN-1-C. SP-GFP-SUN-1-C protein is composed of GFP and the C terminus of SUN-1 encompassing the coiled coil and SUN domain which are located in the perinuclear space. It has dominant interfering effects and displaces Nesprins from the nuclear envelope by competing with endogenous SUN proteins for binding to the Nesprin KASH domains. An N-terminal signal peptide (SP) derived from torsin A ensures targeting of the fusion protein to the ER and the perinuclear space.[32] SP-GFP, a fusion protein comprising the signal peptide of torsin and GFP, was used as a control. Nesprin-2 was successfully displaced from the NE and the cells were then employed in independent experiments for live imaging (**Fig. 6A**). Ca^{2+} measurements demonstrate a 3-fold increase in Rhod-2 related fluorescence in the cytoplasm of SP-GFP-SUN-1-C expressing cells as compared to SP-GFP expressing cells, indicating that displacing Nesprins from the nuclear envelope results in elevated cytoplasmic Ca^{2+} levels (**Fig. 6B, C**).

Differential expression of Nesprin-2 in ovarian cancer cell lines and its effect on nuclear transport

SKOV-3 and Caov-3 are human ovarian adenocarcinoma cell lines. Intriguingly, they express variable amounts of Nesprin-2. Nesprin-2 is greatly reduced in Caov-3 cells as compared to SKOV-3 cells as shown by protein gel blot and immunofluorescence analysis (**Fig. 7A, B**). For the analysis we used pAbK1 antibodies. In SKOV-3 we detected proteins of >400 kDa, ~250 kDa and ~90 kDA whereas Caov-3 cells expressed low amounts of the >400 kDa, no ~250 kDa protein and low amounts of the 90 kDa protein with pAbK1. In immunofluorescence analysis these antibodies stained strongly the NE in SKOV-3 cells, whereas in Caov-3 cells no NE staining

Displacing Nesprins from the nuclear envelope results in increased cytoplasmic Ca^{2+} concentrations

Cellular Ca^{2+} has a crucial role in regulating nuclear transport.[18] In order to investigate the effect of loss of Nesprins on

was detected. Instead, a diffuse cytosolic staining was seen. Corresponding to the Nesprin-2 reduction, Caov-3 cells showed reduced nuclear BRCA1. In fact, BRCA1 was diffusely distributed throughout the cells. By contrast, in SKOV-3 cells BRCA1

is predominantly nuclear (**Fig. 7B**). Strikingly, Rhod-2 analysis showed elevated cytoplasmic Ca^{2+} levels in Caov-3 cells in comparison to SKOV-3 cells (**Fig. 7C, D**).

Loss of Nesprin-2 in EDMD5 fibroblasts results in reduced BRCA1 nuclear localization and enhanced cytoplasmic Ca^{2+}

It has been shown that the mutation in Nesprin-2β in EDMD5 resulted in loss of Nesprin-2 from the NE.[24] In agreement with previously published data, we found a strongly reduced Nesprin-2 staining in patient fibroblasts carrying the T89M mutation as compared to control fibroblasts. In addition in the EDMD5 fibroblasts we observed a diffuse BRCA1 staining throughout the cell and no nuclear enrichment as in the control (**Fig. 8A**). This could be due to abnormal nuclear trafficking in the EDMD5 fibroblasts. Subsequent Ca^{2+} measurements showed elevated cytoplasmic Ca^{2+} levels in the EDMD5 fibroblasts as compared to control fibroblasts (**Fig. 8B, C**).

Discussion

Here we further elucidate the role for Nesprin-2 in nuclear transport and suggest that it might be Ran independent and Ca^{2+}/Calmodulin dependent. We further point out potential implications for ovarian adenocarcinoma and EDMD5.

Nesprin-2 KD cells have abnormal transport of c-Fos and Smad 2/3 in response to TGF β stimulation. This in
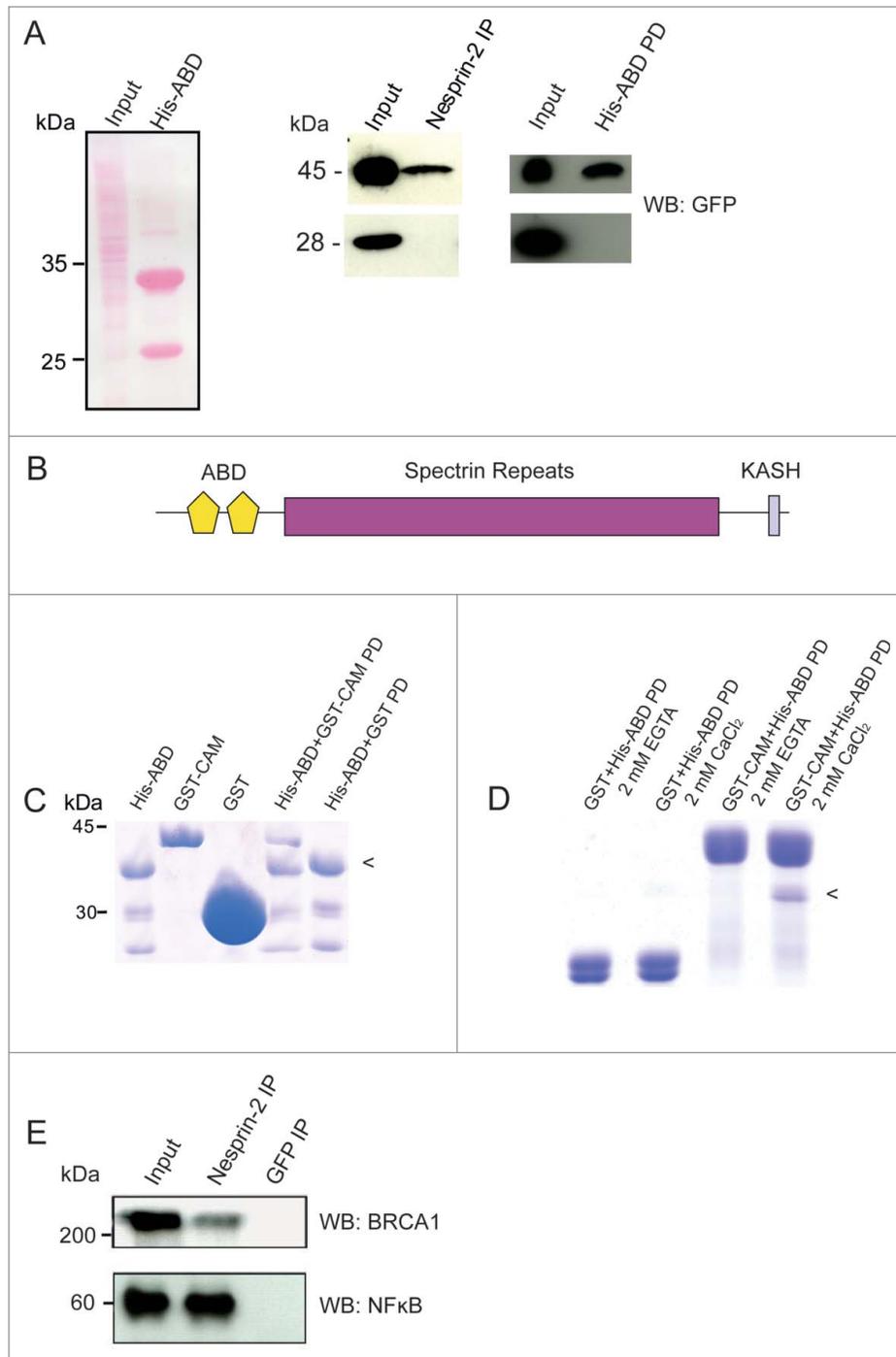

Figure 5. Nesprin-2 interacts with Calmodulin, BRCA1 and NF-κB. (**A**) Left panel, Ponceau S stained gel showing the HaCaT cell lysate (Input) used for pull down and immunoprecipitation and the His-ABD polypeptide (~33 kDa). The smaller band at ~25 kDa is presumably a breakdown product. Middle panel, detection of YFP-Calmodulin (45 kDa) in the Nesprin-2 immunoprecipitate (IP) using pAbK1. Right panel, detection of YFP-Calmodulin in the His-ABD pull down (PD). The panels below show the control pulldowns with cells expressing YFP (28 kDa). Detection was with mAb K3–184–2. (**B**) Domain structure of Nesprin-2 showing the localization of the ABD composed of 2 CH domains, the rod domain made from spectrin repeats and the C-terminal KASH domain which harbors a transmembrane domain. (**C**) Direct interaction of the Nesprin-2 ABD and Calmodulin. His-ABD bound to Ni-NTA beads was incubated with GST-Calmodulin (GST-CAM) or GST for control. PD, pull down. (**D**) For analyzing the Ca^{2+} dependence of the interaction, His-ABD released from beads was incubated with GST-calmodulin bound to beads in the presence of Ca^{2+} or its absence (+EGTA). The arrowhead in (C) and (D) points to the position of His-ABD. (**E**) Coimmunoprecipitation of BRCA1 and NF-κB from HaCaT cell lysates (Input) with Nesprin-2 antibodies pAbK1 (IP). mAb K3–184–2 against GFP was used for control. The resulting blots were probed with BRCA1 and NFκB specific antibodies, respectively.
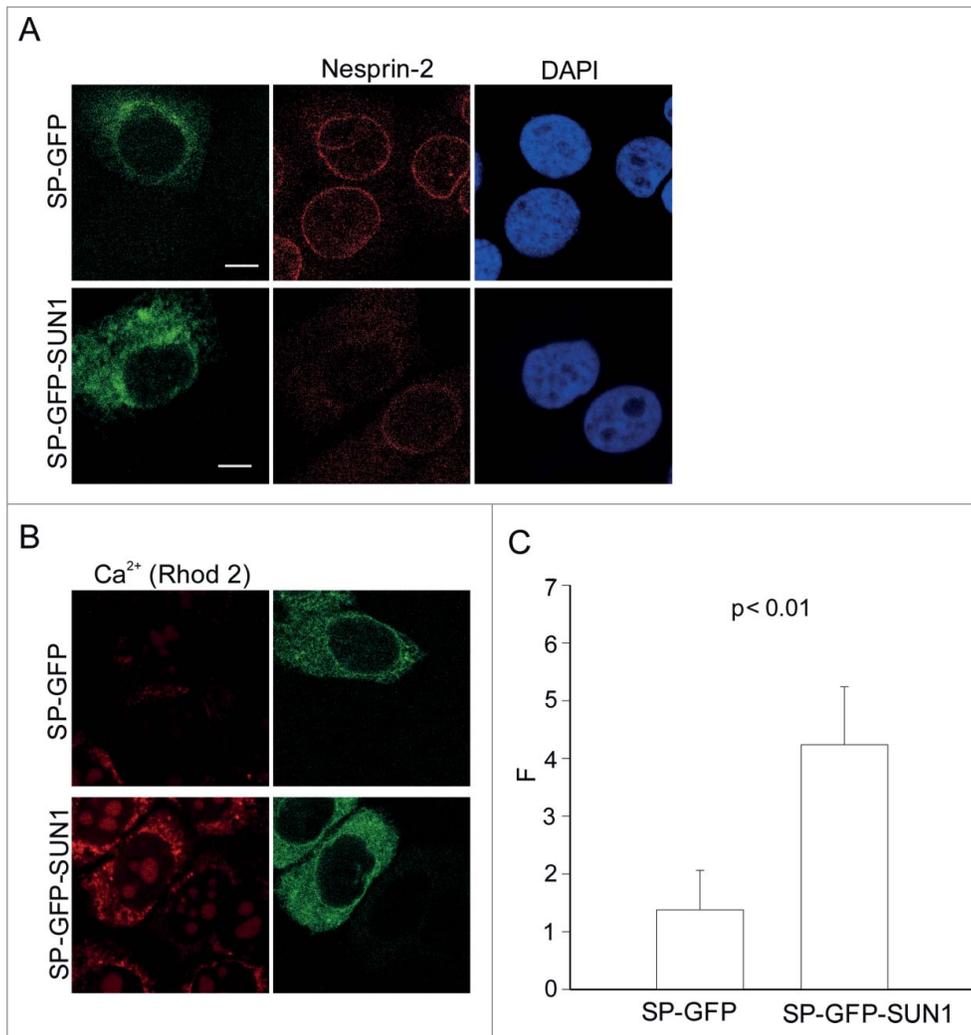
Figure 6. Ca^{2+} imaging in cells expressing SP-GFP-SUN1-C. (**A**) Effect of SP-GFP-SUN1-C polypeptide interfering with Nesprin localization in a dominant manner. HaCaT cells were transfected either with control SP-GFP plasmid or SP-GFP-SUN1-C plasmid. Immunofluorescence analysis was performed using pAbK1 Nesprin-2 antibodies and DAPI. (**B**) Representative image of live transfected cells loaded with Rhod-2. (**C**) Quantitative comparison of fluorescence measurements in the transfected cell lines (F: corrected Rhod-2 fluorescence intensity): The values represent mean and SD of 3 independent experiments (p value, 0.0021). 50 cells were analyzed.

turn has an effect on keratinocyte proliferation and wound healing.[23] Here we show that in addition to c-Fos and Smad 2/3, Nesprin-2 KD cells have abnormal BRCA1 and NF-κB transport. Strikingly, we observe abnormal BRCA1 localization in the ovarian adenocarcinoma cell line Caov-3 and EDMD5 fibroblasts, similar to what is observed in Nesprin-2 KD cells.

BRCA1 and NF-κB as substrates for the Ca^{2+}/Calmodulin pathway

BRCA1 nuclear transport is Ca^{2+} regulated, i.e., enhancing cytoplasmic Ca^{2+} promotes nuclear export of BRCA1 and chelating intracellular Ca^{2+} favors nuclear accumulation of BRCA1.[11] We found that Calmodulin-YFP overexpression led to a diffuse BRCA1 localization throughout the cell, whereas in YFP overexpressing cells BRCA1 remained nuclear (data nor shown). We

identified a novel binding site between the NLS containing region of BRCA1 and Calmodulin. Taken together, our data supports previous findings of the dependence of BRCA1 localization on the Ca^{2+}/Calmodulin pathway.[11] We further identified a novel interaction between Nesprin-2 and Calmodulin. Considering the model suggested by Hanover et al. (2009), we propose that Nesprin-2 could be a candidate protein that can act as a receptor for Ca^{2+}/Calmodulin bound cargo.[2] Based on its reported localization near nuclear pore complexes Nesprin-2 may then facilitate or enhance nuclear import.[30] The depletion of Nesprin-2 after shRNA mediated knockdown results in the failure of the recognition of the Ca^{2+}/Calmodulin bound cargo for nuclear trafficking resulting in abnormal localization. Further, Nesprin-2 knockdown cells have a hypoactive DDR as shown by reduced γ-H2AX foci. DDR entails trafficking of proteins from one subcellular compartment to the other. Our results suggest that hypoactive DDR can be attributed to the failure of nuclear localization of several factors that are not concentrated in the nuclear compartment upon Nesprin-2 depletion. Whether RNA trafficking is also affected in addition to protein trafficking is not known so far.

Elevated cytoplasmic levels of Ca^{2+} upon loss of Nesprin-2

Elevated cytoplasmic levels of Ca^{2+} upon loss of Nesprin-2 are intriguing and may explain the pathogenesis of EDMD. An increase in intracellular Ca^{2+} in Duchenne muscular dystrophy (DMD) is a well-known factor playing an important role in cardiomyopathy in DMD.[33] However, important limitations of the experiment have to be recognized. SP-GFP-SUN-1-C plasmid although an important tool for live cell imaging, has a major drawback. In addition to displacing Nesprin-2 it also displaces Nesprin-1 making it difficult to conclude whether the enhanced cytoplasmic Ca^{2+} is due to Nesprin-2 loss alone or a combined effect of loss of Nesprin-2 and Nesprin-1 from the nuclear envelope. However, the finding is very significant as it indicates the importance of NE proteins in a dual function, namely Ca^{2+} physiology and Calmodulin binding both of which impact on nuclear trafficking. Strikingly, this finding is also replicated in
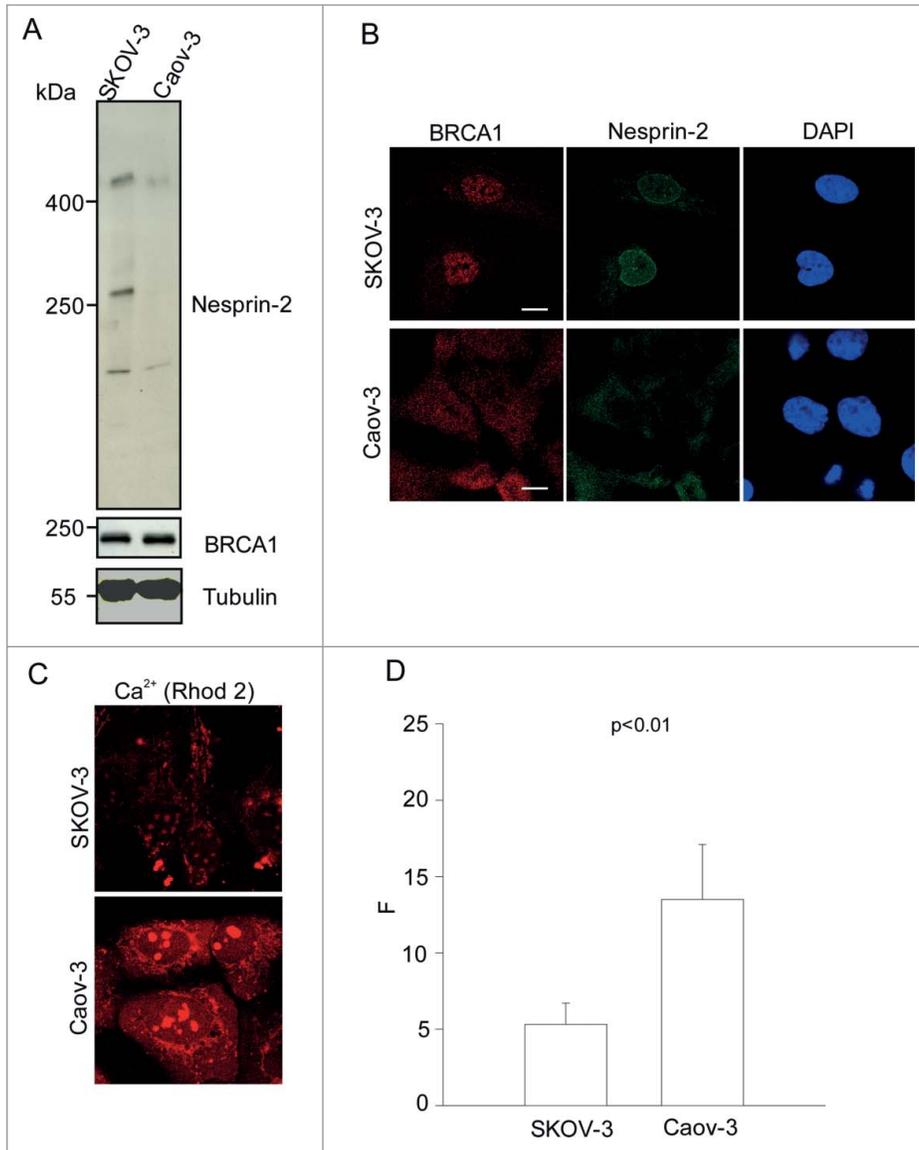
Figure 7. Nesprin-2 expression, BRCA1 localization and steady-state Ca^{2+} in ovarian adenocarcinoma cell lines SKOV-3 and Caov-3. (**A**) Western blot analysis using lysates obtained from SKOV-3 and Caov-3 cells and probed with pAbK1 for Nesprin-2 and BRCA1 antibodies. The proteins were separated in a 3–10%- gradient gel. YL1/2 antibodies were used to detect β-tubulin. (**B**) Immunofluorescence analysis performed on SKOV-3 and Caov-3 cells using BRCA1 antibodies, Nesprin-2 pAbK1 antibodies and DAPI. (**C**) Representative images of SKOV-3 and Caov-3 cells loaded with Rhod-2 to detect steady state cytoplasmic Ca^{2+}. (**D**) Quantitative comparison of fluorescence measurements in the 2 cell lines (F: corrected Rhod-2 fluorescence intensity). The values represent mean and SD of 3 independent experiments (p value, 0.0076). 100 cells were analyzed.

adenocarcinoma and EDMD5. Further studies should focus on the effect of Ca^{2+} chelators, Ca^{2+} release inhibitors and molecules interfering with Calmodulin kinase effects on nuclear transport, DDR and cell survival in the abovementioned cells. Unfortunately, the clinical data from the patients from whom the ovarian tumor cells have been derived is not available. It would be necessary to investigate the relation between Nesprin-2 expression and tumor properties like metastasis, invasion and tumor growth.

Experimental Procedures

Cell culture

The human keratinocyte cell line (HaCaT), COS7 and ovarian adenocarcinoma cell lines were cultured in DMEM medium (PAN Biotech No. P04–03550) with high glucose (4,5 g/dL), penicillin/streptomycin, glutamate and 5% fetal bovine serum. The ovarian adenocarcinoma cell lines were a kind gift from Prof. Baki Akgül (Institute of Virology, Medical Faculty, University of Cologne).[34,35] Cells were grown in a humidified atmosphere and 5% CO_2. Subcutaneous fibroblasts from a patient suffering from EDMD5 were a gift from Prof. Wehnert (Institute of Human Genetics and Interfaculty Institute of Genetics and Functional Genomics, University Greifswald).[24] The fibroblasts (Passage 13–17) were cultivated in Eagle's MEM (Gibco, No. 31095–029), 20% fetal bovine serum, 7.5% Bicarbonate, 1 M HEPES, penicillin-streptomycin and glutamate.

Immunofluorescence analysis

Cells were seeded on coverslips (12 mm diameter). After the desired treatment they were fixed using 3% paraformaldehyde, permeabilized with 0.5% Triton X-100 and blocked with phosphate buffered gelatin (PBG). For monoclonal antibodies against BRCA1 methanol fixation was used. Rabbit polyclonal antibodies pAbK1 (1:250) and mouse monoclonal mAb K20–478 (1:250)[26,30] specific for Nesprin-2, rabbit polyclonal antibodies against NF-κB (1:300, Abcam), polyclonal and monoclonal antibodies against BRCA1 (Abcam, 1:200 for the mAb) and mAb414 (Abcam) against nuclear pore complex proteins were diluted in PBG and the cells were incubated with

the clinical models. The ovarian adenocarcinoma cell line Caov-3 that has reduced Nesprin-2 expression as compared to SKOV-3 also has elevated cytoplasmic Ca^{2+}, and EDMD5 fibroblasts which show Nesprin-2 mislocalization also show elevated Ca^{2+} levels.

Clinical relevance

Our results suggest that the role of Nesprin-2 in Ca^{2+}/Calmodulin mediated nuclear trafficking can be exploited for treating ovarian
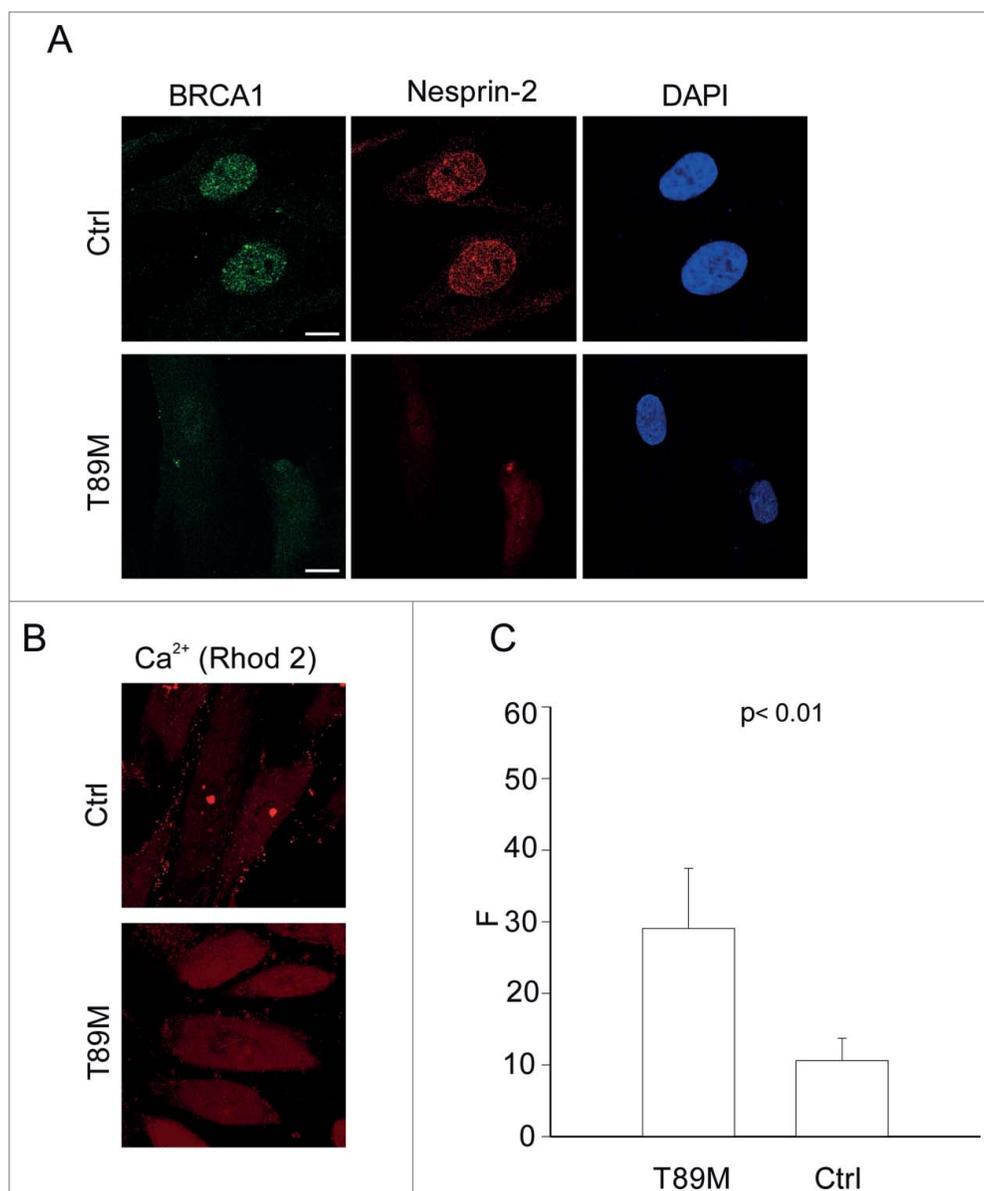
Figure 8. Mislocalization of BRCA1 and elevated cytoplasmic Ca²⁺ in EDMD5 fibroblasts. (**A**) Immunofluorescence analysis of control (Ctrl) and patient fibroblasts (T89M) carrying a mutation in Nesprin-2β using Nesprin-2 specific pAbK1 and BRCA1 specific antibodies. Scale bar, 10 μM. (**B**) Representative image of control and patient fibroblasts loaded with Rhod-2. (**C**) Quantitative comparison of fluorescence measurement in control and patient fibroblasts (F: corrected Rhod-2 fluorescence intensity). The values represent mean and SD of 3 independent experiments (p value, 0.0074). 50 cells were analyzed.

UV induced DNA damage

The cells were exposed to 80 J/m² UVC using a Hoefer UV transilluminator. After UV exposure, the cells were briefly washed with PBS and incubated with fresh media for 4 h and processed for immunofluorescence.

Immunoprecipitation

Cells were trypsinized and pelleted. The cells were lysed using lysis buffer (50 mM Tris-HCl, pH 7.0, 0.5% sodium desoxycholate, 1% NP40, 150 mM NaCl, 1 mM DTT, proteinase inhibitor cocktail). The lysate was passed through a syringe and needle (0.4 mm gauge) 10 times and sonicated at 20% amplitude. The lysate was then centrifuged at 12,000 rpm and the supernatant incubated with Protein A Sepharose beads for one hour (preclearing). The precleared lysate was centrifuged and the supernatant incubated with antibodies (3–5 μg/ml) for 2 h. This mixture was then incubated overnight with Protein A Sepharose beads. All reactions were performed at 4° C. The next day the beads were pelleted and washed with ice-cold PBS and the beads finally boiled with 2x SDS sample buffer at 95° C. The supernatant was loaded onto SDS polyacrylamide gels (12% acrylamide and 3–10%- gradient gel to probe for Nesprin-2).

GST and His tag pull down assay

Plasmids encoding various regions of BRCA1 expressed as GST fusion proteins, namely, PGEXT2tkcs BRCA1 (aa 1–324), (aa 341–748), (aa 262–553) and (aa 504–802) were obtained from Prof. Steve Elledge.[38] The actin-binding domain of Nesprin-2 was expressed as His tag fusion (His-ABD).[30] GST or His tagged fusion proteins were expressed in *E. coli* XL1 blue. Bacteria were grown to an OD₆₀₀ between 0.6 and 0.8 and protein expression overnight at 20°C was induced by the addition of 0.5 mM Isopropyl-1-thio-D-galactopyranoside (IPTG). The bacteria were harvested, washed and lysed with STE buffer (10 mM Tris-HCl, pH 8.0, 50 mM NaCl, 1 mM EDTA) supplemented with protease

primary antibodies for 2 hours. Cells were washed with PBS and subsequently incubated with appropriate secondary antibodies conjugated to Alexa 488 or 568 (Sigma) along with DAPI to stain the DNA for 45 min. Coverslips were washed and fixed on slides using Gelvatol. Images were taken using a confocal microscope (Leica). SV40-NLS-PK plasmid was a kind gift from Prof. Pavel Hozak, Institute of Molecular Genetics of the ASCR.[5] The γ-H2AX foci were analyzed using cellprofiler image analysis software.[36,37] Foci ≥0 .7 μm were counted.

inhibitors (Sigma). Lysis was performed by mechanical shearing with a Dounce homogenizer in the presence of 100 μg/ml lysozyme followed by 15 min incubation on ice. Lysates from bacteria expressing GST fusion proteins were additionally supplemented with Sarkosyl to a final concentration of 1.5%. All samples were sonicated and centrifuged at 16.000 rpm for 30 min. Supernatants were transferred to a new tube and lysates from bacteria expressing GST fusion proteins were supplemented with Triton X-100 to a final concentration of 2%. GST and His-tag fusion proteins were purified from bacterial lysates by adding glutathione Sepharose 4B (GE Healthcare) or Ni-NTA beads (Qiagen) as required at 4°C for 4 hours. Beads were washed 5 times with PBS to remove non-specifically bound proteins. His-ABD was eluted from Ni-NTA beads with 250 mM imidazole, Calmodulin-GST or GST bound to GST-Sepharose beads were released using glutathione. Eluted proteins were dialyzed against 50 mM Tris-HCl, pH 7.5. For interaction studies beads bound proteins and the putative binding partner were incubated for 4 hours at 4 degrees in 50 mM Tris-HCl, pH 7.5, 100 mM NaCl, 10 % Glycerol, 0.05% Triton X-100. The beads were extensively washed and the beads bound proteins analyzed by SDS-PAGE. To study a dependence on Ca^{2+} the incubation was carried out in the presence of 2 mM $CaCl_2$ or 2 mM EGTA.

COS7 cells expressing Calmodulin-YFP or YFP or GFP as indicated were lysed with lysis buffer (50 mM Tris-HCl, pH 7.5, 150 mM NaCl, 1% Nonidet-P40, and 0.5% sodium deoxycholate) supplemented with protease inhibitors. For pre-clearing, lysates of COS7 cells expressing YFP fusion proteins were incubated with beads for one hour at 4°C followed by incubation with the corresponding GST- or Ni-NTA beads bound fusion proteins for 3 hours. For probing a Ca^{2+} dependency of the interaction, the incubation was carried out in the presence of 2 mM $CaCl_2$ or 2 mM EGTA. Finally, beads were washed 5 times with PBS supplemented with protease inhibitors. SDS sample buffer was added and samples were heated for 5 min at 95°C and analyzed by SDS-PAGE followed by Coomassie Blue staining or western blot analysis. β-actin as loading control was recognized using monoclonal antibodies (Sigma). YFP-fusion proteins were detected with mAb K3–184–2. YL1/2 antibodies were used for β-tubulin detection serving as control.

Knock-down of Nesprin-2 using shRNA

Human Nesprin-2 shRNAs were constructed as duplexes with the sequence Nesprin-2 C-terminal (N2C2)-5′CCAGC CTCCTGCAACATCCGAAGCTTGGGATGTTGCAGGAG GCTGGTTTTTT 3′ and the control5′ATCTACTCGACGT GAGCGTGAAGCTTGACGCTCACGTCGAGTAGATTTT TT 3′. HaCaT cells were transfected twice at intervals of 3 d using the Amaxa cell line Nucleofector® kit V (Lonza) according to the manufacturer's instructions. Cells were seeded on the plate and fresh media was added 24 hours after seeding. Cells were analyzed after overnight incubation.

Calcium imaging

Cells were plated on IBIDI plates (Martinsried). Prior to live Ca^{2+} imaging, they were washed twice with KRH buffer (125 mM NaCl, 5 mM KCl, 1.8 mM $CaCl_2$, 2.6 mM $MgSO_4$, 5 mM Hepes, pH 7.2). Then they were incubated with Rhod-2 acetoxymethyl (AM) ester (Life technologies) (1μM) reconstituted in KRH buffer for 20 min. Cells were washed 6 times with KRH buffer and incubated in KRH for a further 20 minutes at room temperature to allow complete deesterification of Rhod-2 AM. Images were obtained using a Leica confocal microscope (SP5) (63X and 100 X magnifications for SP-GFP and ovarian adenocarcinoma cell lines respectively). Image analysis was done using ImageJ software as follows. A square field was chosen where there were no cells. Intensity (gray scale value) was measured and this was regarded as F0, in arbitrary units (background intensity). Similar square field area gray scale measurements were taken for cells loaded with calcium and their individual intensity taken as F. Background correction was calculated as F-F0. Average values of background corrected intensity were taken for the cells measured. At least 3 independent experiments were performed. The graph and statistics was performed using Sigmaplot software.[39]

References

1. Hanover JA, Love DC, DeAngelis N, O'Kane ME, Lima-Miranda R, Schulz T, Yen YM, Johnson RC, Prinz WA. The High Mobility Group Box Transcription Factor Nhp6Ap enters the nucleus by a calmodulin-dependent, Ran-independent pathway. J Biol Chem 2007; 282(46):33743-51; PMID:17878171; http://dx.doi.org/10.1074/jbc.M705875200

2. Hanover JA, Love DC, Prinz WA. Calmodulin-driven nuclear entry: trigger for sex determination and terminal differentiation. J Biol Chem 2009; 284(19):12593-97; PMID:19126540; http://dx.doi.org/10.1074/jbc.R800076200

3. García-Palmero I, Villalobo A. Calmodulin regulates the translocation of Grb7 into the nucleus. FEBS Lett 2012; 586(10):1533-39; http://dx.doi.org/10.1016/j.febslet.2012.04.017

4. Antonsson A, Hughes K, Edin S, Grundstrom T. Regulation of c-Rel nuclear localization by binding of Ca^{2+}/calmodulin. Mol Cell Biol 2003; 23(4):1418-27; PMID:12556500; http://dx.doi.org/10.1128/MCB.23.4.1418-1427.2003

5. Dzijak R, Yildirim S, Kahle M, Novak P, Hnilicova J, Venit T, Hozak P. Specific nuclear localizing sequence directs two myosin isoforms to the cell nucleus in calmodulin-sensitive manner. PLoS one 2012; 7(1): e30529; PMID:22295092; http://dx.doi.org/10.1371/journal.pone.0030529

6. Argentaro A, Sim H, Kelly S, Preiss S, Clayton A, Jans DA, Harley VR. A SOX9 defect of calmodulin-dependent nuclear import in campomelic dysplasia/autosomal sex reversal. J Biol Chem 2003; 278(36):33839-47; PMID:12810722; http://dx.doi.org/10.1074/jbc.M302078200

7. Kaur G, Delluc-Clavieres A, Poon IK, Forwood JK, Glover DJ, Jans DA. Calmodulin-dependent nuclear import of HMG-box family nuclear factors: importance of the role of SRY in sex reversal. Biochem J 2010; 430(1):39-48; PMID:20528776; http://dx.doi.org/10.1042/BJ20091758

8. Kaur G, Lieu KG, Jans DA. 70-kDa heat shock cognate protein hsc70 mediates calmodulin-dependent nuclear import of the sex-determining factor SRY. J Biol Chem 2013; 288(6):4148-57; PMID:23235156; http://dx.doi.org/10.1074/jbc.M112.436741

9. Sim H, Argentaro A, Harley VR. Boys, girls and shuttling of SRY and SOX9. Trends Endocrinol Metab 2008; TEM 19(6):213-22; PMID:18585925; http://dx.doi.org/10.1016/j.tem.2008.04.002

10. Gao W, Zhu H, Zhang JY, Zhang XJ. Calcium signaling-induced Smad3 nuclear accumulation induces acetylcholinesterase transcription in apoptotic HeLa cells. Cell Mol Life Sci 2009; 66(13):2181-93; PMID:19468687; http://dx.doi.org/10.1007/s00018-009-0037-z

11. Glover-Collins K, Thompson ME. Nuclear export of BRCA1 occurs during early S phase and is calcium-dependent. Cell Signal 2008; 20(5):958-68; PMID:18296025; http://dx.doi.org/10.1016/j.cellsig.2008.01.007

12. Sée V, Rajala NK, Spiller DG, White MR. Calcium-dependent regulation of the cell cycle via a novel MAPK–NF-kappaB pathway in Swiss 3T3 cells. J Cell Biol 2004; 166(5):661-72; http://dx.doi.org/10.1083/jcb.200402136

13. Stehno-Bittel L, Perez-Terzic C, Clapham DE. Diffusion across the nuclear envelope inhibited by depletion of the nuclear Ca^{2+} store. Science 1995; 270 (5243):1835-8; PMID:8525380; http://dx.doi.org/10.1126/science.270.5243.1835

14. Greber UF, Gerace L. Depletion of calcium from the lumen of endoplasmic reticulum reversibly inhibits passive diffusion and signal-mediated transport into the nucleus. J Cell Biol 1995; 128(1-2):5-14; PMID:7822421; http://dx.doi.org/10.1083/jcb.128.1.5

15. Holaska JM, Black BE, Rastinejad F, Paschal BM. Ca^{2+}-dependent nuclear export mediated by calreticulin. Mol Cell Biol 2002; 22(17):6286-97; PMID:12167720; http://dx.doi.org/10.1128/MCB.22.17.6286-6297.2002

16. Berchtold CM, Wu ZH, Huang TT, Miyamoto S. Calcium-dependent regulation of NEMO nuclear export in response to genotoxic stimuli. Mol Cell Biol 2007; 27(2):497-509; PMID:17074802; http://dx.doi.org/10.1128/MCB.01772-06

17. Schlumm F, Mauceri D, Freitag HE, Bading H. Nuclear calcium signaling regulates nuclear export of a subset of class IIa histone deacetylases following synaptic activity. J Biol Chem 2013; 288(12):8074-84; PMID:23364788; http://dx.doi.org/10.1074/jbc.M112.432773

18. Sweitzer TD, Hanover JA. Calmodulin activates nuclear protein import: a link between signal transduction and nuclear transport. Proc Natl Acad Sci U S A 1996; 93(25):14574-9; PMID:8962094; http://dx.doi.org/10.1073/pnas.93.25.14574

19. Rajgor D, Shanahan CM. Nesprins: from the nuclear envelope and beyond. Expert Rev Mol Med 2013; 15: e5; PMID:23830188; http://dx.doi.org/10.1017/erm.2013.6

20. Lüke Y, Zaim H, Karakesisoglou I, Jaeger VM, Sellin L, Lu W, Schneider M, Neumann S, Beijer A, Munck M, et al. Nesprin-2 Giant (NUANCE) maintains nuclear envelope architecture and composition in skin. J Cell Sci 2008; 121 (Pt 11):1887-98; PMID:18477613; http://dx.doi.org/10.1242/jcs.019075

21. Meinke P, Nguyen TD, Wehnert MS. The LINC complex and human disease. Biochem Soc Trans 2011; 39 (6):1693-7; PMID:22103509; http://dx.doi.org/10.1042/BST20110658

22. Lombardi ML, Jaalouk DE, Shanahan CM, Burke B, Roux KJ, Lammerding J. The interaction between nesprins and sun proteins at the nuclear envelope is critical for force transmission between the nucleus and cytoskeleton. J Biol Chem 2011; 286(30):26743-53; PMID:21652697; http://dx.doi.org/10.1074/jbc.M111.233700

23. Rashmi RN, Eckes B, Glockner G, Groth M, Neumann S, Gloy J, Sellin L, Walz G, Schneider M, Karakesisoglou I, et al. The nuclear envelope protein Nesprin-2 has roles in cell proliferation and differentiation during wound healing. Nucleus 2012; 3(2):172-86; PMID:22198684; http://dx.doi.org/10.4161/nucl.19090

24. Zhang Q, Bethmann C, Worth NF, Davies JD, Wasner C, Feuer A, Ragnauth CD, Yi Q, Mellad JA, Warren DT, et al. Nesprin-1 and -2 are involved in the pathogenesis of Emery Dreifuss muscular dystrophy and are critical for nuclear envelope integrity. Hum Mol Genet 2007; 16 (23):2816-33; PMID:17761684; http://dx.doi.org/10.1093/hmg/ddm238

25. Sur I, Neumann S, Noegel AA. Nesprin-1 role in DNA damage response. Nucleus 2014; 5(2):173-91; PMID: 24781983; http://dx.doi.org/10.4161/nucl.29023

26. Libotte T, Zaim H, Abraham S, Padmakumar VC, Schneider M, Lu W, Munck M, Hutchison C, Wehnert M, Fahrenkrog B, et al. Lamin A/C-dependent localization of Nesprin-2, a giant scaffolder at the nuclear envelope. Mol Biol Cell 2005; 16(7):3411-24; PMID:15843432; http://dx.doi.org/10.1091/mbc.E04-11-1009

27. Henderson BR. The BRCA1 Breast Cancer Suppressor: Regulation of Transport, Dynamics, and Function at Multiple Subcellular Locations. Scientifica 2012; 2012:796808; PMID:24278741

28. Sharma A, Singh K, Almasan A. Histone H2AX phosphorylation: a marker for DNA damage. Methods Mol Biol 2012; 920:613-26; PMID:22941631; http://dx.doi.org/10.1007/978-1-61779-998-3_40

29. Lange A, Mills RE, Lange CJ, Stewart M, Devine SE, Corbett AH. Classical nuclear localization signals: definition, function, and interaction with importin α. J Biol Chem 2007; 282(8):5101-5; PMID:17170104; http://dx.doi.org/10.1074/jbc.R600026200

30. Zhen YY, Libotte T, Munck M, Noegel AA, Korenbaum E. NUANCE, a giant protein connecting the nucleus and actin cytoskeleton. J Cell Sci 2002; 115(Pt 15):3207-3222; PMID:12118075

31. Ribeiro Ede A, Jr., Pinotsis N, Ghisleni A, Salmazo A, Konarev PV, Kostan J, Sjoblom B, Schreiner C, Polyansky AA, Gkougkoulia EA, et al. The structure and regulation of human muscle α-actinin. Cell 2014; 159 (6):1447-1460; PMID:25433700; http://dx.doi.org/10.1016/j.cell.2014.10.056

32. Neumann S, Schneider M, Daugherty RL, Gottardi CJ, Eming SA, Beijer A, Noegel AA, Karakesisoglou I. Nesprin-2 interacts with {α}-catenin and regulates Wnt signaling at the nuclear envelope. J Biol Chem 2010; 285(45):34932-8; PMID:20801886; http://dx.doi.org/10.1074/jbc.M110.119651

33. van Westering TL, Betts CA, Wood MJ. Current understanding of molecular pathology and treatment of cardiomyopathy in Duchenne muscular dystrophy. Molecules 2015; 20(5):8823-55; PMID:25988613; http://dx.doi.org/10.3390/molecules20058823

34. Fogh S. [Letter: Diagnosis of malaria]. Ugeskr Laeger 1975; 137(51):3045-6; PMID:1198755

35. Hamilton TC, Young RC, McKoy WM, Grotzinger KR, Green JA, Chu EW, Whang-Peng J, Rogan AM, Green WR, Ozols RF. Characterization of a human ovarian carcinoma cell line (NIH:OVCAR-3) with androgen and estrogen receptors. Cancer Res 1983; 43 (11):5379-89; PMID:6604576

36. Carpenter AE, Jones TR, Lamprecht MR, Clarke C, Kang IH, Friman O, Guertin DA, Chang JH, Lindquist RA, Moffat J, et al. CellProfiler: image analysis software for identifying and quantifying cell phenotypes. Genome Biol 2006; 7(10):R100

37. Lamprecht MR, Sabatini DM, Carpenter AE. CellProfiler: free, versatile software for automated biological image analysis. Biotechniques 2007; 42(1):71-5; PMID:17076895; http://dx.doi.org/10.2144/000112257

38. Cortez D, Wang Y, Qin J, Elledge SJ. Requirement of ATM-dependent phosphorylation of brca1 in the DNA damage response to double-strand breaks. Science 1999; 286(5442):1162-6; PMID:10550055; http://dx.doi.org/10.1126/science.286.5442.1162

39. Cheng H, Lederer WJ, Cannell MB. Calcium sparks: elementary events underlying excitation-contraction coupling in heart muscle. Science 1993; 262 (5134):740-4; PMID:8235594; http://dx.doi.org/10.1126/science.8235594